Smart Structures and Systems, *Vol. 29, No. 1 (2022) 17-28*
https://doi.org/10.12989/sss.2022.29.1.017

Damaged cable detection with statistical analysis, clustering, and deep learning models

Hyesook Son [1], Chanyoung Yoon [1], Yejin Kim [1], Yun Jang*[1], Linh Viet Tran [2], Seung-Eock Kim [2], Dong Joo Kim [2] and Jongwoong Park [3]

[1] *Department of Computer Engineering and Convergence Engineering for Intelligent Drone, Sejong University, 209 Neungdong-ro, Gwangjin-gu , Seoul, Republic of Korea*
[2] *Department of Civil and Environmental Engineering, Sejong University, 209, Neungdong-ro, Gwangjin-gu, Seoul, Republic of Korea*
[3] *School of Civil and Environmental Engineering, Urban Design and Studies, Chung-Ang University, 84 Heukseok-ro, Dongjak-gu, Seoul, Republic of Korea*

(*Received March 21, 2021, Revised September 29, 2021, Accepted October 4, 2021*)

Abstract. The cable component of cable-stayed bridges is gradually impacted by weather conditions, vehicle loads, and material corrosion. The stayed cable is a critical load-carrying part that closely affects the operational stability of a cable-stayed bridge. Damaged cables might lead to the bridge collapse due to their tension capacity reduction. Thus, it is necessary to develop structural health monitoring (SHM) techniques that accurately identify damaged cables. In this work, a combinational identification method of three efficient techniques, including statistical analysis, clustering, and neural network models, is proposed to detect the damaged cable in a cable-stayed bridge. The measured dataset from the bridge was initially preprocessed to remove the outlier channels. Then, the theory and application of each technique for damage detection were introduced. In general, the statistical approach extracts the parameters representing the damage within time series, and the clustering approach identifies the outliers from the data signals as damaged members, while the deep learning approach uses the nonlinear data dependencies in SHM for the training model. The performance of these approaches in classifying the damaged cable was assessed, and the combinational identification method was obtained using the voting ensemble. Finally, the combination method was compared with an existing outlier detection algorithm, support vector machines (SVM). The results demonstrate that the proposed method is robust and provides higher accuracy for the damaged cable detection in the cable-stayed bridge.

Keywords: anomaly detection; clustering; deep learning; LSTM; time series

1. Introduction

The importance of structural health monitoring (SHM) is continuously increasing to ensure the safety and durability of large infrastructure such as tunnels, bridges, and plants. One of key factors in the SHM is to identify any damage correctly and quickly within structures for the purpose of preventing the catastrophic collapses and failure of infrastructure requiring considerable socio-economic losses. Cable-stayed bridges among various infrastructure are quite expensive and would be easily deteriorated because they are generally located in marine environments. Stayed cable is the most important element of the cable-stayed bridge and significantly influences structural integrity as it directly transmits the load of the bridge deck to the pylons. A small damage of stayed-cables may generate significant deterioration of overall bridge systems by losing the load-carrying capacity of bridges (Jo *et al*. 2011).

Many researchers have more attention to SHM techniques for evaluating structural status via statistical modeling and machine learning, such as clustering. Recently, several studies to detect structure damages in statistical modeling were performed by extracting Damage Sensitive Features (DSFs) from time-series data. Models such as Autoregressive Moving Average Model (ARMA), which are time series models, and AutoRegressive Moving Average models with eXogenous inputs (ARMAX), were employed to calculate the DSFs from time-series data. Nair *et al*. (2006) modeled the vibration signal of the ASCE benchmark structure using ARMA. They defined the DSF utilizing three AR coefficients in the ARMA model. The DSF average of the damaged vibration data is significantly different from one of the healthy operating structures. Yu and Lin (2017) calculated the residuals of the time-series model with the ARMA model and define the DSF as the ratio of the residual. Structure damage tests with the DSF were carried out employing a three-story building structure. If the DSF value obtained from the structure channels is greater than 1, it is determined that the channel is damaged. As a result of the experiment, the DFS value increases as the nonlinear damage severity increases. Entezami *et al*. (2020) extracted features in the data collected from sensors attached to a cable-stayed bridge with an ARMA model. The extracted features have been used in the Partition-based

*Corresponding author, Ph.D., Professor,
E-mail: jangy@sejong.edu

ISSN: 1738-1584 (Print), 1738-1991 (Online)

Kullback-Leibler Divergence (PKLD) and the nearest neighbor (NN) rule (PKLD-NN) method. They judged that the element of the bridge is damaged when the distance value obtained by the PKLD-NN is higher than the threshold. Mei and Gül (2015) define the DFS using ARMAX to identify structural stiffness and mass changes. The variables used in the DFS definition are the coefficients in the ARMAX model. They assumed that any damage to a part of the structure would affect the surroundings as well. The changes in stiffness and mass were discovered, and the degree was depicted in the DFS value. Catbas *et al*. (2012) estimated the effect of the damaged structure with cross-correlation. They detected outliers using cross-correlation of sensor data collected from the bridge. The cross-correlation between the sensors was calculated, and a mean correlation matrix was generated. They identified the structural damage by the difference matrix representing the difference between the mean correlation matrices of the normal and damaged structures.

In addition to defining the DFS from the data, there are techniques for separating seasonal and trend fluctuations to analyze time-series data. Seasonal and Trend decomposition using Loess (STL), one of the statistical models for analyzing time-series data, explains the trend fluctuations representing long-term changes from time-series data and seasonal fluctuations that change periodically. The STL model has been applied to detect events or outliers in social media. Chae *et al*. (2013) extracted the topics of abnormal events from social media and then decomposed the topic volumes using the STL model. Lee and Kim (2018) predicted the data after a specific time point t with the SARIMA model from time-series data, calculated the difference between the actual value and the predicted value, and then perform the STL decomposition. Finally, they extracted the remainder data by removing the trend component and the seasonal component from the time-series data to identify the outliers and intervals where anomalies occur.

Various clustering techniques have been proposed to identify outliers in machine learning. Zhang *et al*. (2010) presented a classification and comparison table for the methodology to estimate outliers in wireless sensor networks. They reported statistical techniques, nearest-neighbor-based approaches, clustering methods, classification methods, and spectral decomposition-based approaches for estimating outliers. Among them, the clustering methods do not require any prior knowledge of the data distribution. However, it is not easy to select appropriate parameters, and it is pointed out that it is expensive to calculate the distances between data records in multivariate data. Duan *et al*. (2019) provided a new definition of outliers as the process of detecting data records that are significantly different or inconsistent with the rest of the dataset. Besides, they noticed that not only single data but also one cluster could be an outlier. Jiang and An (2008) reported a clustering-based outlier detection method. They explained that outlier detection aims to discover rare and very exceptional data compared to other data. They also described how to create a dataset grouped by a clustering algorithm and determine outlier clusters from the created data. Pamula *et al*. (2011) utilized the K-means clustering to discover outliers. Since the data records near the center of each cluster cannot be outliers, they removed these data records from the cluster and calculate the outlier scores based on the distance. They indicated the data record with the highest score as an outlier. Alamdari *et al*. (2017) presented a new approach to detecting outliers, such as structural damage and system problems in a large infrastructure that is continuously monitored. They applied a spectral-based technique based on the measured spectral moment (SM) to identify ordinary and damaged signals. After that, the modified k-means clustering algorithm was applied to the data to detect an abnormal response. Diez *et al*. (2016) presented a clustering-based technique for substructures or joints with similar bridge motions. They performed a combination of feature extraction and outlier removal and then cluster the data to classify damaged joints.

Deep learning models are devised for training complex nonlinear correlations within datasets. When sufficient data is available for the network training, the deep learning models perform best in various tasks such as nonlinear feature extraction, classification, regression, and anomaly detection. Deep learning has been widely applied to detect structural damages. Pathirage *et al*. (2018) trained a deep autoencoder (DAE) to predict the steel frame structure state with modal information such as frequencies and mode shapes. They generated training data with an updated finite element model and apply supervised learning to predict the stiffness parameters representing the impairment state. They showed that the proposed method enables efficient dimension reduction and accurate damage prediction. Gu *et al*. (2017) proposed a multilayer artificial neural network (ANN) that detects structural damages through unsupervised learning. To eliminate the effect of temperature on fluctuations in frequencies, they utilized the frequencies and temperature data into the ANN input data. Target data had the same frequencies as the input data, and they calculated the Euclidean distance between the ANN output and the target data for the anomaly detection. The ANN was trained only with data extracted from the undamaged structure. Therefore, when the Euclidean distance increases, it is possible to distinguish data from the damaged structure. Since this work has no ground truth data, the structural damages can only be detected through unsupervised learning, like a deep learning model for outlier detection.

Outlier detection in time-series data is also possible using deep learning models. Malhotra *et al*. (2016) proposed a Long Short-Term Memory Networks based Encoder-Decoder architecture for Anomaly Detection (EncDec-AD) that detects anomalies in multi-sensor time-series such as data collected from sensors mounted on mechanical devices. EncDec-AD was trained to reconstruct target sequence data identical to the input sequence data. Since they train the EncDec-AD with a 'normal' time-series that do not contain outliers, they detected sections with high reconstruction errors as anomalous sequences. However, they only detected when an outlier occurs but do not identify which sensor causes the outlier. Zhang *et al*. (2019) proposed a Multi-Scale Convolutional Recurrent Encoder-

Decoder (MSCRED) that diagnoses outliers in multivariate time-series data. They created a signature matrix representing the inter-correlations of two time-series pairs as input data for MSCRED. MSCRED consists of a convolutional encoder that captures a spatial pattern of signature matrices, an attention-based convolutional LSTM (Xingjian *et al*. 2015) that catches temporal dependencies, and a convolutional decoder that reconstructs the same signature matrix as the input data. The trained MSCRED detects in which time steps it contains outliers. Given the detection results, they ranked the anomaly scores of each time series using the prediction error. Furthermore, they identified specific ranking series as sensors causing outliers. As presented in Malhotra *et al*. (2016) and Zhang *et al*. (2019), in this work, a deep learning model was trained to classify damaged cables by identifying data with high prediction errors as outliers.

In this paper, three different methodologies are applied to detect the damaged cable and compare the results to confirm the actual damaged cable. Fig. 1 illustrates the proposed modeling process with time-series analysis, time-series clustering, and deep learning. The data provided by the International Project Competition for Structural Health Monitoring (Bao *et al*. 2021) are utilized, and various models and visualization techniques are implemented to validate that proposed methods are appropriate. Finally, the stay cable named SJS11 is determined as the damaged cable.

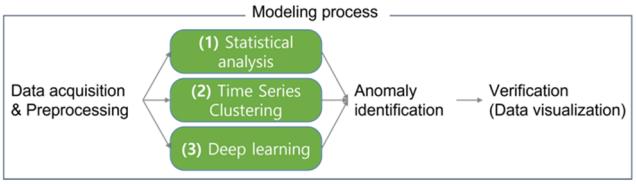

Fig. 1 Proposed modeling process for the damaged cable identification in the cable-stayed bridge

2. Data description and data preprocessing

This study utilizes the data provided by the International Project Competition for Structural Health Monitoring (Bao *et al*. 2021). Cable tension was monitored at a double tower and double cable-plane cable-stayed bridge in China. This cable-stayed bridge consists of 168 cables, and each cable is given a name according to the rules. The cables are numbered as 1-21 toward the direction of the bank and river from the tower. N or S is assigned depending on whether it is North or South side, and A or J is assigned according to whether it is on the bank or river side. Moreover, S or X is assigned according to whether it is up or downstream. The tension data were collected from the 14 cables, SJS08 to SJS14 and SJX08 to SJX14. The data were captured for ten days, from 2006-05-13 to 2006-05-19, 2007-12-14, 2009-05-05, and 2011-11-01. The data sampling frequency was 2 Hz, and 172,800 tension data records were stored per day from one cable. One of 14 cables was known as damaged in 2011. In this study, the damaged cable is identified based on the measurement dataset using the three approaches mentioned in the introduction.

Fig. 2 shows the tension of 14 cables for 10 considered days. As seen in the figure, there are outliers every hour in the SJS13 data between 2007 and 2011. The outliers in SJS13 occurred exactly every 3,600 seconds. Therefore, the outliers of SJS13 are considered as generated by other causes such as data communication, not cable damage, and these outliers are removed using the interquartile range (IQR), the difference between first quartile Q1 and third quartile Q3. The data records smaller than Q1-1.5 × IQR or above Q3 + 1.5 × IQR are judged as outliers. Furthermore, the deleted values are substituted by linear interpolation. Given two coordinates, (x_1, x_2) and (y_1, y_2), the linear interpolation constructs new data using the following linear polynomial.

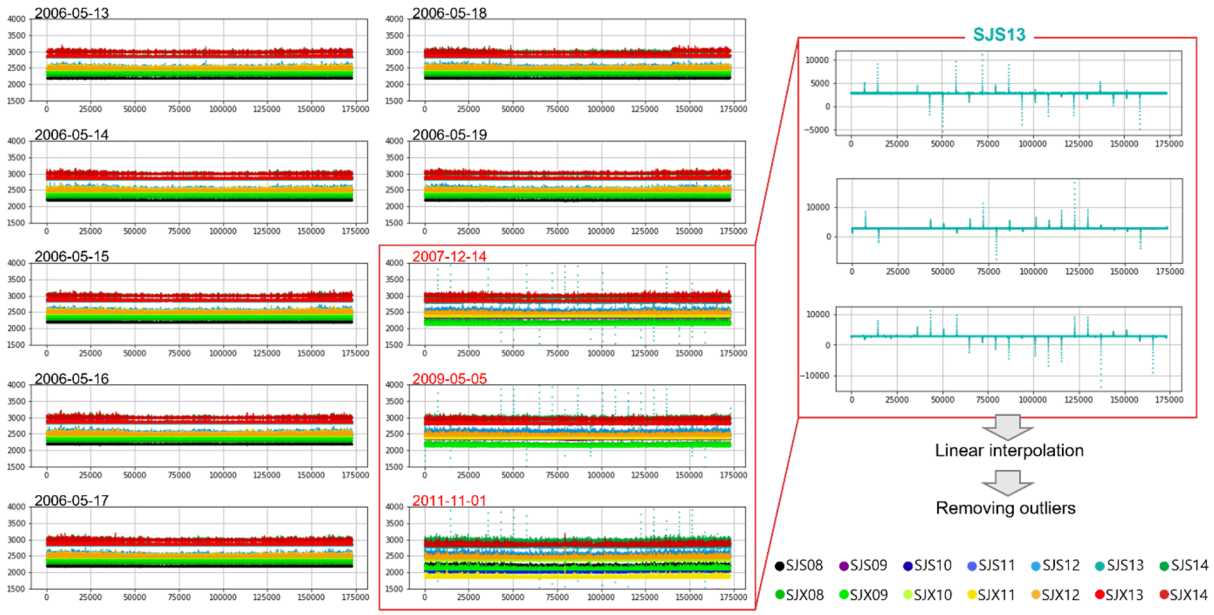

Fig. 2 Tension data for 10 days

$$y = y_1 + (x - x_1)\frac{y_2 - y_1}{x_2 - x_1} \quad (1)$$

It is possible to interpolate the deleted values with two points. However, since the first data record on 2007-12-14 is identified as an outlier, and only one point is given, there is a part that is not interpolated. Therefore, the first 90 samples and the last 90 samples for each of the 14 days data must be removed. Consequently, there are 172,620 tension data samples included in each day after the preprocessing.

Since the cable tension data is affected by sensor error, external load, environmental effect, and zero-shift of sensors, Li *et al*. (2018) decomposed the raw tension T_t as follows.

$$T_t = T_D + T_E + T_V + T_R,$$

where, T_D, T_E, and T_V are factors of tension affected by dead load, environmental effect, and vehicles, respectively, and T_R is negligible noise. Tian *et al*. (2020) calculated the temperature effect and detrend the tension data by applying the moving average. They subtracted the temperature effect from the original data and extract only the data that is affected by the vehicle load. Similarly, after removing outliers from the cable data, the moving average, one of the Low Pass Filters, is applied to obtain the data without the effects of sensor fault and external load. Therefore, it is possible to capture tension changes affected by the vehicle influence only. The sensor errors and damage conditions are identified by discovering outliers for cables with patterns different from intact cables.

T_V is utilized to discover the cable where the sensor error occurred. This study assumes that if an error occurs in the cable sensor, the decomposed T_V will appear as an outlier. Fig. 3(a) shows the decomposed T_V after applying a low pass filter to the data on November 1, 2011. It is observed that T_V values of most cables are distributed between -50 kN and 300 kN. However, as shown in Fig. 3(b), the T_V values of SJS13 are distributed between -50 kN and 50 kN in 2007, 2009, and 2011. Fig. 3(c) presents that the T_V of SJX08 is distributed between -0.5 kN and 1 kN in 2011, and Fig. 3(d) reveals that although the T_V of SJX13 goes up to 20 kN around 11:30 pm on November 11, 2011, most T_V values are distributed between -0.5 kN and 1 kN, similar to ones of SJX08. From these figures, it is found that the cable tension data of SJS13 has different signal patterns from one of the other cables. Moreover, the cable tensions of SJX08 and SJX13 have small values and value changes compared to other cables. Therefore, SJS13, SJX08, and SJX13 are classified as outliers where sensor errors occurred in the cables, and the cables SJX08, SJS13, and SJX13 with sensor failure are excluded in the further abnormal cable detection models.

3. Methodology 1: Time series analysis approach

3.1 STL model

The Seasonal and Trend decomposition using Loess (STL) model is a technique for decomposing time-series data into trend, seasonality, and remainder (Cleveland *et al*. 1990). The STL has the characteristic of making robust sub-series because it is suitable for outlier processing. Since the STL treats the decomposition results of neighboring time points independently, it does not limit the seasonality pattern to have a specific form, allowing the STL to decompose time series data using various frequency sets, such as day, months, or quarters (Theodosiou 2011). The STL is achieved through local regression (LOESS) smoothing. The LOESS indicates the local regression about a point. The STL consists of two loops. Robustness weights are obtained in the outer loop, whereas the trend and seasonal components are repeatedly updated in the inner loop. The trend component indicates how the time series data increases or decreases in the long run. The seasonal component refers to repeated patterns with a specific period in time-series data. The remainder is a component after removing the trend and seasonal components from time-

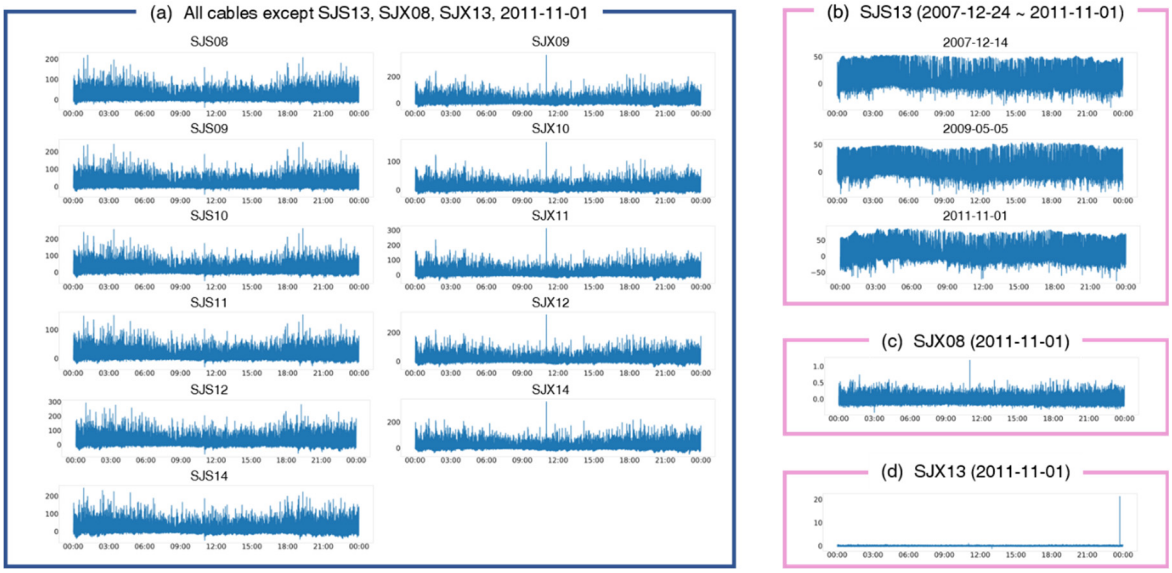

Fig. 3 LPF passed tension data

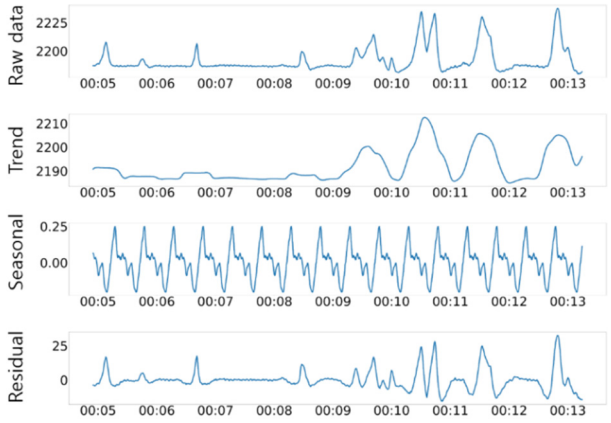

Fig. 4 Decomposition plot of SJS08 on 2006-05-13

series data. Cleveland *et al*. (1990) remarked that the frequency of an appropriate seasonal component in STL depends on the series characteristics. The tension data are divided into segments representing single-vehicle-induced tension as proposed in the study by Li *et al*. (2018). The average time for one vehicle to cross the bridge is about 25.04 seconds. Therefore, 30 seconds is enough time for the vehicle to pass, and the seasonal frequency is set to 60. The statsmodels library in python is utilized to decompose the seasonality. When using the library, the sequence periodicity is set to 60, and default values are applied for the remaining parameters. Fig. 4 shows the STL decomposition for the tension data of SJS08 for 9 minutes on May 13, 2006. The figure presents the original, trend, seasonal, and remainder signals from top to bottom. The trend component shows that the tension of SJS08 becomes smoothed compared to the raw data. The seasonal component represents the pattern of the tension value for SJS08 every 30 seconds.

3.2 Damaged cable extraction using STL model

In this section, the original time-series data is decomposed using the STL decomposition, and the damaged cable is identified by examining the cross-correlations of the decomposed tension values. The data is preprocessed, as mentioned in the above section. After applying the STL decomposition to 11 cable data that do not have any sensor errors, the cross-correlation is computed between cables with the remainder data from which the trend component and the seasonal component are removed.

The cross-correlation is calculated as follows.

$$(f * g)[n] \overset{def}{=} \sum_{m=-\infty}^{\infty} f^*[m]g[m+n] \tag{2}$$

where, f and g denote time series data. As f and g are similar, the cross-correlation value increases. It is assumed that the average cross-correlation value between the damaged cable and its neighbor cables differs from one between the normal cable and its neighbor cables. Fig. 5 shows the average cross-correlation between one cable and other cables located on both sides and the opposite side of this cable. The cross-correlation is calculated with all cables except for the cable with sensor faults. The average cross-correlation of SJS14 must be the average of cross-correlation with the adjacent cable SJS13 and cross-correlation with the opposite cable SJX14. However, since SJS13 has a sensor fault, the cross-correlation for SJS14 is only calculated between SJS14 and SJX14. Similarly, the cross-correlation of SJX14 is computed between SJX14 and SJS14 since SJX13 has a sensor fault. Therefore, in Fig. 5, the SJX14 graph overlaps the SJS14 graph, which means one of them is not visible because the cross-correlation of SJS14 is the same as one of SJX14. The average cross-correlation values significantly increase for all 11 cables between May 5, 2009, and November 1, 2011. The average cross-correlation increases from 2007 because the max of the remainder is larger than in 2006. The max of the remainder in 2006 is 100 kN. However, the max of the remainder in 2007 and 2009 becomes 150 kN, and the max of the remainder in 2011 is 200 kN. When calculating the cross-correlation between two-time series in Eq. (2), the cross-correlation increases as the values of the time series data increase. The average increase rate of 11 cables is 99.54%, of which the average cross-correlation increase rate of SJS11 is the lowest at 34.11%. Therefore, the cable SJS11 is judged as the damaged cable since it has the smallest increase in cross-correlation. When SJS11 was damaged in 2011, the correlation with undamaged cables, SJS10, SJS12, and SJX11, is low, and since the correlation is low, the increase rate of the average cross-correlation for SJS11 is lower than the ones for other cables. An additional experiment was performed to identify damaged cables by changing the seasonal frequency for STL decomposition under the same conditions. Table 1 shows the average cross-correlation change from May 5, 2009, to November 1, 2011, by changing the seasonal frequency. As shown in the table, the cross-correlation change of SJS11 is the smallest regardless of the seasonal frequency.

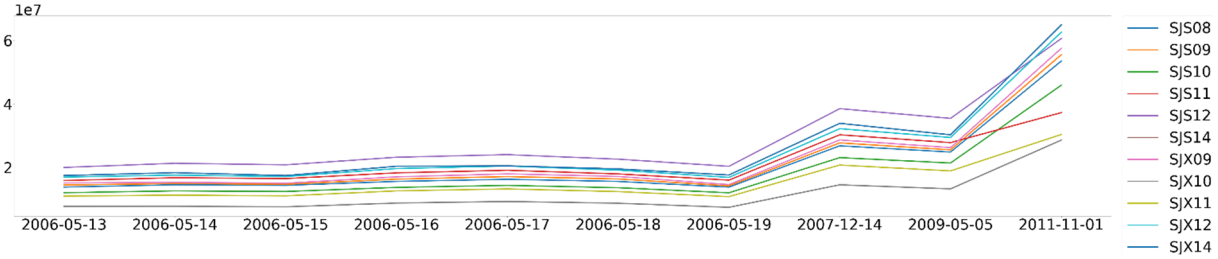

Fig. 5 Mean cross-correlation

Table 1 Effect of seasonality frequency on average cross-correlation change between May 5, 2009, and November 1, 2011

	Seasonal frequency				
	50	60	120	180	240
SJS08	108.60	115.92	110.73	107.41	108.78
SJS09	111.24	117.87	114.13	111.39	113.46
SJS10	110.16	115.21	111.03	109.03	111.10
SJS11	**31.80**	**34.11**	**31.98**	**31.46**	**32.42**
SJS12	68.74	71.20	69.03	68.36	69.11
SJS14	112.57	114.84	116.04	112.54	112.65
SJX09	113.75	119.71	117.35	115.21	117.95
SJX10	112.88	116.95	115.80	115.80	116.00
SJX11	59.29	61.12	62.21	63.43	63.99
SJX12	110.61	113.14	112.61	114.43	113.23
SJX14	112.57	114.84	116.04	112.54	112.65

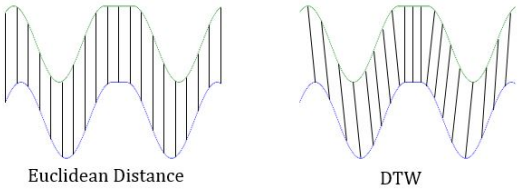

Fig. 6 Comparison of DTW and Euclidean distance calculation methods

4. Methodology 2: Time series clustering

4.1 Clustering

Clustering refers to the process of grouping similar data and dividing the data into n groups. The degree of similarity is measured with the distance between data records, and the distance calculation techniques include Euclidean distance and Dynamic Time Warping (DTW) distance. The Euclidean distance is computed as follows.

$$\overline{AB} = \sqrt{(x_2 - x_1)^2 + (y_2 - y_1)^2}. \quad (3)$$

where x and y are the coordinates of each data point. However, if the time step of time-series data is changed, the Euclidean distance may change as well, which indicates that the Euclidean distance may not be suitable for the clustering of time-series data whose time step might be changed. The DTW distance is utilized to compute the similarity between time-series data by checking whether the current data flow matches the past data flow. The DTW distance is calculated as follows.

$$DTW(x,y) = \min_{\pi} \sqrt{\sum_{(i,j)\in\pi} d(x_i, y_i)^2} \quad (4)$$

Here, x and y are time-series data, d is the distance between x and y, and π is a path that minimizes the Euclidean distance between time-series data. That is, the value of x is compared with the value of y, and the closest point is selected. In this way, the distance calculation makes it possible to measure the distance between two data whose time, speed, and length are not correctly aligned, as shown in Fig. 6.

K-means Time Series Clustering is a method of clustering Time Series Data using K-means. K-means is a grouping method by having one central point for each group and assigning data to the nearest center point as follows.

$$\arg\min_{S} DTW_k(x,y), \quad (5)$$

where S is a set of similar data, and k is the number of sets. The distance between two points in the time series data is calculated with Eq. (4). The goal is to find a set S that minimizes the DTW distance for each set. K-means clustering repeats the Expectation step to allocate data to

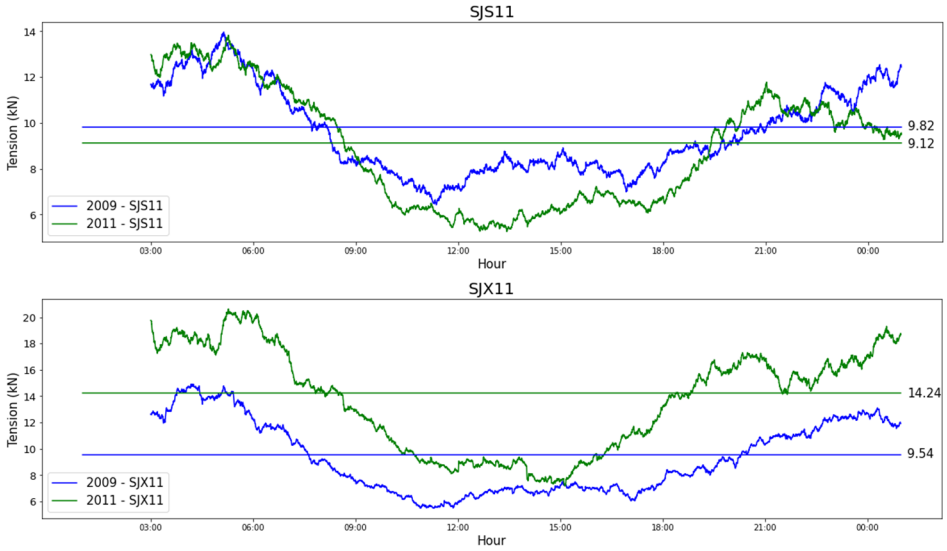

Fig. 7 Moving average (window = 14400) and average graph of SJS11 and SJX11 tension data in 2009 and 2011

the nearest center point and the Maximization step to update the center point to match the boundary of the group.

4.2 Tension ratio clustering

When the cable is damaged, the tension applied to the damaged side decreases. Accordingly, the reduced tension affects the opposite side of the cable, which is expected to increase the tension. Fig. 7 shows the average and moving average graphs of the tension data in 2009 and 2011 for SJS11 and SJX11f among the preprocessed data through the low pass filter. The average tension for SJS11 decreased from 9.82 kN in 2009 to 9.12 kN in 2011, and the average tension for SJX11 increased from 9.54 kN in 2009 to 14.24 kN in 2011, which infers that the damaged cable affects the opposite cable. Therefore, if the tension ratio of the damaged cable and the opposite cable is calculated, it is expected that the damaged cable will show a significant difference compared to other cables. In this study, the tension ratio of one cable and the opposite cable is calculated from the preprocessed data through the low pass filter for clustering. Since SJX08 and SJX13 were excluded from the preprocessing, it is impossible to obtain the tension ratio for SJS08 and SJS13. Therefore, the tension ratios are computed for the cables SJ*09, SJ*10, SJ*11, SJ*12, and SJ*14. Note that SJ* indicates both SJS and SJX. The tension ratio is computed by dividing the upstream side cable (SJS) by the downstream side cable (SJX).

The DTW is utilized as the clustering distance calculation method. However, since the DTW calculates all the distance combinations of (x_i, y_i), it requires a vast amount of memory, which is the square of the data size. Therefore, the average technique is applied to reduce the size of the training data. Since the data shape is 172,620, the average of every 432 data, which is a factor of 172,620, is taken and then, the shape is reduced to 400 in total.

Table 2 presents the clustering results using the tension ratio. For n = 2 and 3, the cables SJ*09 in 2007-2011 and the cables SJ*11 in 2011 are classified into clusters differently from other cables. Therefore, it is inferred that SJS09 or SJX09 has been damaged since 2007, or SJS11 or SJX11 had been damaged in 2011. Table 3 shows the DTW distance between the cluster center and each tension ratio data. In each cell, the DTW distance for n = 2 and the DTW distance for n = 3 are separated by "/". In Cluster 3, since there is no cable classified when n = 2, it is marked with "*". The light blue indicates clusters when n = 2, and the green indicates clusters when n = 3. For example, on 2011-11-01, when n = 2, SJS11 is classified as Cluster 1 because the DTW distance between the center of Cluster 1 and tension ratio data of SJS11 is 12, and the DTW distance between the center of Cluster 2 and tension ratio data of SJS11 is 47. Also, when n = 3, SJS11 is classified as Cluster

Table 2 Tension ratio clustering results

	n = 2	n = 3
Cluster 1	SJ*09 (2007 ~ 2011) SJ*11 (2011)	SJ*09 (2007 ~ 2011)
Cluster 2	All other cables	SJ*11 (2011)
Cluster 3	-	All other cables

Table 3 DTW distance between each cluster center and tension ratio data

DTW Distance between Cluster 1 and tension ratio data (n = 2/n = 3)										
	2006-05-13	2006-05-14	2006-05-15	2006-05-16	2006-05-17	2006-05-18	2006-05-19	2007-12-14	2009-05-05	2011-11-01
SJ*09	68 / 58	68 / 58	68 / 58	69 / 58	68 / 58	68 / 58	68 / 57	6 / 1	6 / 1	37 / 0
SJ*10	70 / 59	70 / 59	69 / 59	70 / 59	69 / 59	70 / 59	69 / 59	59 / 48	52 / 41	54 / 44
SJ*11	97 / 87	97 / 87	97 / 87	98 / 88	97 / 87	97 / 87	97 / 86	74 / 64	67 / 57	12 / 62
SJ*12	64 / 54	64 / 53	63 / 52	63 / 53	62 / 52	63 / 52	63 / 52	60 / 49	54 / 43	55 / 45
SJ*14	82 / 72	82 / 72	81 / 70	80 / 70	78 / 67	69 / 57	88 / 77	90 / 80	73 / 63	48 / 37
DTW Distance between Cluster 2 and tension ratio data (n = 2/n = 3)										
	2006-05-13	2006-05-14	2006-05-15	2006-05-16	2006-05-17	2006-05-18	2006-05-19	2007-12-14	2009-05-05	2011-11-01
SJ*09	1 / 119	1 / 119	1 / 119	1 / 119	1 / 120	1 / 119	2 / 118	60 / 52	62 / 50	118 / 54
SJ*10	1 / 121	2 / 120	2 / 120	1 / 121	1 / 120	1 / 121	2 / 120	8 / 110	11 / 103	9 / 105
SJ*11	11 / 148	11 / 148	10 / 148	10 / 149	11 / 149	11 / 148	10 / 147	1 / 125	2 / 119	47 / 2
SJ*12	4 / 115	4 / 114	3 / 113	3 / 114	3 / 114	4 / 113	5 / 113	6 / 111	10 / 105	8 / 106
SJ*14	3 / 133	3 / 133	2 / 132	2 / 131	1 / 129	1 / 120	5 / 138	8 / 142	1 / 124	13 / 99
DTW Distance between Cluster 3 and tension ratio data (n = 2/n = 3)										
	2006-05-13	2006-05-14	2006-05-15	2006-05-16	2006-05-17	2006-05-18	2006-05-19	2007-12-14	2009-05-05	2011-11-01
SJ*09	* / 1	* / 1	* / 1	* / 1	* / 1	* / 1	* / 2	* / 60	* / 62	* / 118
SJ*10	* / 1	* / 2	* / 2	* / 1	* / 1	* / 2	* / 2	* / 8	* / 11	* / 9
SJ*11	* / 11	* / 11	* / 10	* / 11	* / 11	* / 10	* / 10	* / 1	* / 2	* / 47
SJ*12	* / 4	* / 4	* / 3	* / 3	* / 3	* / 4	* / 5	* / 6	* / 10	* / 8
SJ*14	* / 3	* / 3	* / 2	* / 2	* / 1	* / 2	* / 7	* / 7	* / 1	* / 13

Table 4 Preprocessing clustering results

	n = 2	n = 3
Cluster 1	SJS08 (2007) SJS11 (2011) SJS13 (2007, 2011) SJX10 (2007, 2011)	SJS11 (2011) SJS13 (2009, 2011) SJX10 (2007, 2011)
Cluster 2	All other cables	SJS08 (2007) SJS09 (2007) SJS12 (2009) SJX10 (2009)
Cluster 3	-	All other cables

2 because the DTW distance with Cluster 1, Cluster 2, and Cluster 3 are 62, 2, and 47, respectively.

4.3 Cable clustering

The cables are clustered using the preprocessed data after the low pass filter to determine the damaged cable among the damaged cable candidates obtained in Section 4.2, as presented in Table 2. Like the tension ratio training, the model is trained with the DTW. Since every 432 data are averaged out, the data shape is reduced to 400.

Table 4 shows the clustering results with the preprocessed data. From the tension ratio clustering, it is noticed that there are damaged cables in 2007-2011. Therefore, the table shows only cables classified into different clusters in 2007-2011. For n = 2, SJS08, SJS13, SJX10 in 2007, and SJS11, SJS13, SJX10 in 2011 are grouped into one cluster. For n = 3, SJX10 in 2007, SJS13 in 2009, SJS11, SJS13, and SJX10 in 2011 are clustered together, and SJS08, SJS09 in 2007, and SJS12 and SJX10 in 2009 are grouped into one cluster. Table 5 shows the DTW distance between the cluster center and each cable tension data while clustering each cable tension data. Following the results in Table 4, the DTW distances of 2007-2011 data are presented.

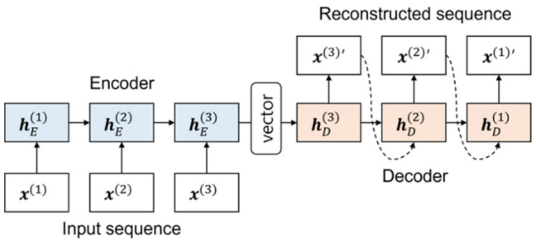

Fig. 8 Encoder-decoder structure

From the results in Tables 2 and 4, the cables SJX09 and SJX11 are intact cables because they are not grouped into different clusters in Table 4. The cable SJS09 is classified into a different cluster in 2007 for n = 3, but it is not classified into a different cluster in 2009 and 2011, which confirms that it is an intact cable. For both n = 2 and 3, the cable SJS11 is classified into different clusters in 2011, which indicates that the cable SJS11 was damaged in 2011.

5. Methodology 3: Deep learning approach

5.1 Long short-term memory networks based encoder-decoder scheme for anomaly detection

Long Short-Term Memory (LSTM) networks (Hochreiter and Schmidhuber 1997) are recurrent neural networks (RNNs) that are widely adopted for time-series data training by catching complex temporal correlations through adjusting the information flow of sequence data. Sutskever *et al.* (2014) propose an Encoder-Decoder network composed of LSTM layers and shows that the long-term dependency can be trained. Fig. 8 shows the Encoder-Decoder structure.

The input data is a time-series with length L, $X = \{\mathbf{x}^{(1)}, \mathbf{x}^{(2)}, \ldots, \mathbf{x}^{(L)}\}$ and $\mathbf{x}^{(i)}$ is a m-dimensional vector. When X is applied to the encoder, the hidden state of

Table 5 DTW distance between each cluster center and tension data

DTW Distance between Cluster 1 and tension ratio data (n = 2/n = 3)												
	SJS08	SJS09	SJS10	SJS11	SJS12	SJS13	SJS14	SJX09	SJX10	SJX11	SJX12	SJX14
2007-12-14	1001 / 1495	1259 / 1420	1293 / 1502	1319 / 1484	1832 / 2129	1268 / 1364	1548 / 1753	1494/ 1698	901 / 717	1400 / 1601	1508 / 1740	1823 / 2005
2009-05-05	1443 / 1109	1455 / 1304	1486 / 1418	1490 / 1372	1700 / 1940	1814 / 1233	1507 / 1597	1415 / 1477	1691 / 1894	1439 / 1407	1430 / 1535	1558 / 1733
2011-11-01	1555 / 1832	1949 / 2340	2093 / 2478	1185 / 1182	2883 / 3468	1859 / 1949	2271 / 2682	2374 / 2849	1107 / 1069	2215 / 2546	2331 / 2703	2658 / 3068
DTW Distance between Cluster 2 and tension ratio data (n = 2/n = 3)												
	SJS08	SJS09	SJS10	SJS11	SJS12	SJS13	SJS14	SJX09	SJX10	SJX11	SJX12	SJX14
2007-12-14	1335 / 1065	1167 / 1173	1291 / 1383	1300 / 1404	1642 / 1766	1732 / 1871	1471 / 1512	1151 / 1482	1577 / 1772	1109 / 1398	1157 / 1514	1470 / 1734
2009-05-05	1065 / 1619	1169 / 1572	1265 / 1593	1239 / 1597	1599 / 1634	1307 / 1995	1411 / 1697	1360 / 1601	913 / 694	1314 / 1660	1392 / 1650	1535 / 1698
2011-11-01	1499 / 1583	1743 / 1944	1793 / 2054	1498 / 1636	2514 / 2866	2195 / 2317	2062 / 2278	2063 / 2372	1512 / 1669	1841 / 2183	1985 / 2330	2380 / 2689
DTW Distance between Cluster 3 and tension ratio data (n = 2/n = 3)												
	SJS08	SJS09	SJS10	SJS11	SJS12	SJS13	SJS14	SJX09	SJX10	SJX11	SJX12	SJX14
2007-12-14	* / 1116	* / 1360	* / 1271	* / 1301	* / 1611	* / 1282	* / 1501	* / 1191	* / 1071	* / 1248	* / 1168	* / 1397
2009-05-05	* / 1069	* / 1188	* / 1247	* / 1234	* / 1702	* / 1387	* / 1403	* / 1347	* / 1108	* / 1267	* / 1328	* / 1522
2011-11-01	* / 1517	* / 1653	* / 1726	* / 1237	* / 2388	* / 1953	* / 2042	* / 2016	* / 1166	* / 1857	* / 1947	* / 2260

LSTM, $H_E = \left\{\mathbf{h}_E^{(1)}, \mathbf{h}_E^{(2)}, \ldots, \mathbf{h}_E^{(L)}\right\}$, is updated, where the dimension of $\mathbf{h}_E^{(i)}$ is the number of LSTM units. The encoder maps the input sequence to a hidden state, which is a vector of fixed dimensions. For the information transfer from the encoder to the decoder, the decoder hidden state is initialized to the last hidden state $\mathbf{h}_E^{(L)}$ of the encoder. There are hidden states, $H_D = \left\{\mathbf{h}_D^{(1)}, \mathbf{h}_D^{(2)}, \ldots, \mathbf{h}_D^{(L)}\right\}$, and the H_D is used to predict the target sequence, which is equivalent to the input sequence. Therefore, the decoder plays the role of reconstructing the vector represented by the encoder as a sequence again. The Encoder-Decoder structure is employed for tasks in various fields such as machine translation, speech recognition, and multiple predictions as it can take a sequence and reconstruct a sequence. Malhotra *et al*. (2016) proposed an outlier detection technique using an LSTM based Encoder-Decoder network. As shown in Fig. 8, they trained EncDec-AD so that the encoder receives the sequence and reconstructs the input sequence in the decoder. Since only normal sequences are used for the EncDec-AD training, they remarked that the reconstruction error will be higher than that of the normal sequences given anomalous sequences. Therefore, they calculated the anomaly score with the network error and detect the segments containing outliers. In this work, the EncDec-AD is trained to determine reconstruction errors and identify the cable data containing outliers.

5.2 Deep learning applied to the cable tension data and results

In this study, the deep learning network is trained with the entire dataset without data labels. The time of high anomaly score is interpreted as the time when the cable is damaged. The anomaly score is defined as follows.

$$a_i = -\log\left(\frac{1}{\sqrt{(2\pi)^m \det\boldsymbol{\Sigma}}}\exp\left(-\frac{1}{2}(\boldsymbol{e}_i - \boldsymbol{\mu})^T\boldsymbol{\Sigma}^{-1}(\boldsymbol{e}_i - \boldsymbol{\mu})\right)\right), \quad (6)$$

where $\boldsymbol{e}_i = |\boldsymbol{x}_i - \boldsymbol{x}_i'|$ is the reconstruction error, and $\boldsymbol{\mu}$ and $\boldsymbol{\Sigma}$ are the parameters in the Normal Distribution $\boldsymbol{e}_i \sim N(\boldsymbol{\mu}, \boldsymbol{\Sigma})$. Therefore, the anomaly score indicates that the data with the most unusual reconstruction errors contain outliers. In order to input each dataset into the LSTM network, the data for ten days are low pass filtered after removing outliers and divided into 60 length intervals. Since the bridge section with sensors is about 300m and 30 seconds is enough time for the vehicle to pass, the sequence length is to 60, which is equivalent to 30 seconds. Therefore, the dataset consists of sequences with 12-dimension with length 60.

The encoder and decoder are configured as one LSTM layer each and set the dimension of hidden states to 8. The model is trained to minimize the mean absolute error of the network using the ADAM optimizer (Kingma and Ba 2015) with a learning rate of 0.0001. The number of epochs is set to 200 and the batch size to 32. The deep learning network is implemented using the Pytorch library (Paszke *et al*. 2017).

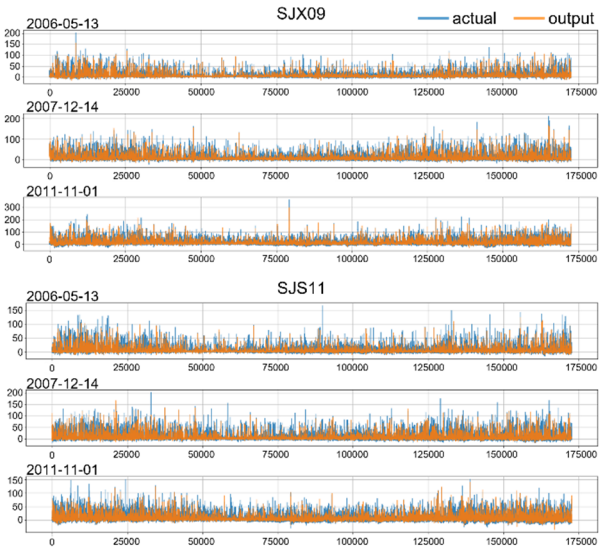

Fig. 9 Results for LSTM training

Fig. 9 represents the predicted values and the actual values as graphs. Table 6 shows the anomaly score for each date. It is observed that the 2011-11-01 data has the highest anomaly score. Since the input data is multivariate time series data, not only the cable data including outliers but also data of other cables are affected, which deteriorates the reconstruction of all cables. Also, as seen in Table 6, it is confirmed that the anomaly scores increased in 2007, 2009, and 2011 compared to 2006. The reason appears that the data for seven consecutive days were obtained in 2006, whereas there was only one-day data in 2007, 2009, and 2011. The tension patterns may change over time, and if there are relatively few data samples each year, the anomaly score may increase. However, since the anomaly score increased the most rapidly and had the largest value in 2011, it is interpreted that the bridge was damaged in 2011. In work by Zhang *et al*. (2019), the series with high reconstruction errors in the outlier segment is identified as an outlier. Similarly, the error of each cable data is computed to identify the cable data with the highest error as an outlier in 2011-11-01 data. Table 7 shows the Root Mean Square Error (RMSE). The error in this study is utilized to classify damaged cables. Since our goal is to select which cable has the highest reconstruction error, the relative error magnitudes are compared. Because the reconstruction error of cable SJS11 cable is the highest, SJS11 is judged as a cable with outlier data.

In the previous studies (Gu *et al*. 2017, Malhotra *et al*. 2016, and Zhang *et al*. 2019), normal data was utilized for training a deep learning model, and abnormal data is used as a test set. This is a reasonable approach when the outliers are very sparse (Malhotra *et al*. 2016). It is assumed that the bridge was not continuously operating with damaged conditions most of the time, especially in the early period

Table 6 Anomaly scores

Date	2006-05-13	2006-05-14	2006-05-15	2006-05-16	2006-05-17
Score	-3.2730	-3.5118	-3.5272	-3.6186	-3.5356
Date	2006-05-18	2006-05-19	2007-12-14	2009-05-05	**2011-11-01**
Score	-2.7490	-3.4255	-1.8070	-1.4346	**-0.2893**

Table 7 RMSE for 2011-11-01 data

Cable	SJS08	SJS09	SJS10	**SJS11**	SJS12	SJS13	SJS14
MAPE	1.2864	1.3800	1.4136	**1.4145**	1.3345	1.2229	1.2009
Cable	SJX08	SJX09	SJX10	SJX11	SJX12	SJX13	SJX14
MAPE	-	1.3051	1.3446	1.3373	1.2906	-	1.1710

(ex. 2006-05-13~2006-05-19). Therefore, the entire data was used for the network learning. Although there is a limitation of assuming that the normal data will be more than the abnormal data, this is a valid assumption in detecting the damaged structure.

6. Discussion

The statistical analysis, the clustering, and the deep learning model are applied to discover the damaged cable. In this section, the outcomes of each approach are reviewed. The STL decomposition model for the statistical time series analysis shows that the SJS11 cable has the lowest increasing rate compared to other cables. The distances of the time series data are also calculated with the Euclidean and DTW, and the K-means time series clustering is applied. In addition, since the damaged cable affects other cables, the tension ratios are estimated between the cables and their opposite cables. Then the clustering algorithm is employed to classify the first set of damaged cable candidates. After that, the preprocessed data are clustered to classify the second set of damaged cable candidates. It is observed that SJS11 is the only cable in the intersection of the first and second sets of damaged candidates. Moreover, the EncDec-AD is utilized for training temporal patterns, and it is discovered that the reconstruction error of SJS11 is the highest in 2011 data. Finally, it is concluded that the SJS11 is the damaged cable since the results of all three techniques consistently report the same cable SJS11. However, the LSTM also classifies the SJS10 as a damaged cable. Furthermore, as shown in Table 7, the LSTM generates the error of SJS10 as high as that of SJS11. In Table 7, since the RMSE increases in the order of SJS08, SJS09, and SJS10, and the RMSE increases in the order of SJS14, SJS13, and SJS12, it is presumed that the closer the cable is to SJS11, the higher the RMSE. Therefore, the RMSE of SJS10 was affected by one of SJS11 because SJS10 was adjacent to the damaged SJS11, and the LSTM does not seem to effectively classify the damaged cable and the intact cable adjacent to the damaged cable.

Instead of detecting damaged cables with a single method, voting ensemble method is employed to incorporate the predicted results from all models comprehensively. The voting ensemble is a learning technique that increases learning efficiency by combining several learning algorithms (Braga *et al*. 2007). The cable with the largest number of votes among the cables listed as damaged by different algorithms will be classified as the final damaged cable in the voting ensemble method. Therefore, damaged cables are distinguished with the voting ensemble every hour in 2011-11-01 data, and Table 8 shows the results. When the cross-correlation technique is applied,

Table 8 Hourly accuracy

Hr.	Cross Corr.	Cluster	LSTM	SVM	Combination
00	SJS11	SJS11	SJS11	SJS11	SJS11
01	SJS11	-	SJS11	SJS11	SJS11
02	SJS11	SJS11	SJS11	-	SJS11
03	SJS11	SJS11	SJS10	SJS11	SJS11
04	SJS11	SJS11	SJS10	-	SJS11
05	SJS11	SJS11	SJS10	SJS11	SJS11
06	SJS11	-	SJS11	SJS11	SJS11
07	SJS11	SJS11	SJS11	SJS11	SJS11
08	SJS11	SJS11	SJS11	-	SJS11
09	SJS11	-	SJS11	-	SJS11
10	SJS11	SJS11	SJS11	SJS11	SJS11
11	SJS11	SJS11	SJS11	SJS11	SJS11
12	SJS11	SJS11	SJS11	-	SJS11
13	SJS11	SJS11	SJS11	SJS11	SJS11
14	SJS11	SJS11	SJS11	SJS11	SJS11
15	SJS11	SJS11	SJS11	SJS11	SJS11
16	SJS11	SJS11	SJS11	SJS11	SJS11
17	SJS11	SJS11	SJS11	-	SJS11
18	SJS11	SJS11	SJS11	-	SJS11
19	SJS11	SJS11	SJS10	-	SJS11
20	SJS11	SJS11	SJS10	-	SJS11
21	SJS11	SJS11	SJS10	-	SJS11
22	SJS11	SJS11	SJS10	-	SJS11
23	SJS11	SJS11	SJS10	SJS11	SJS11
Acc.	100%	87.5%	67%	54.2%	100%

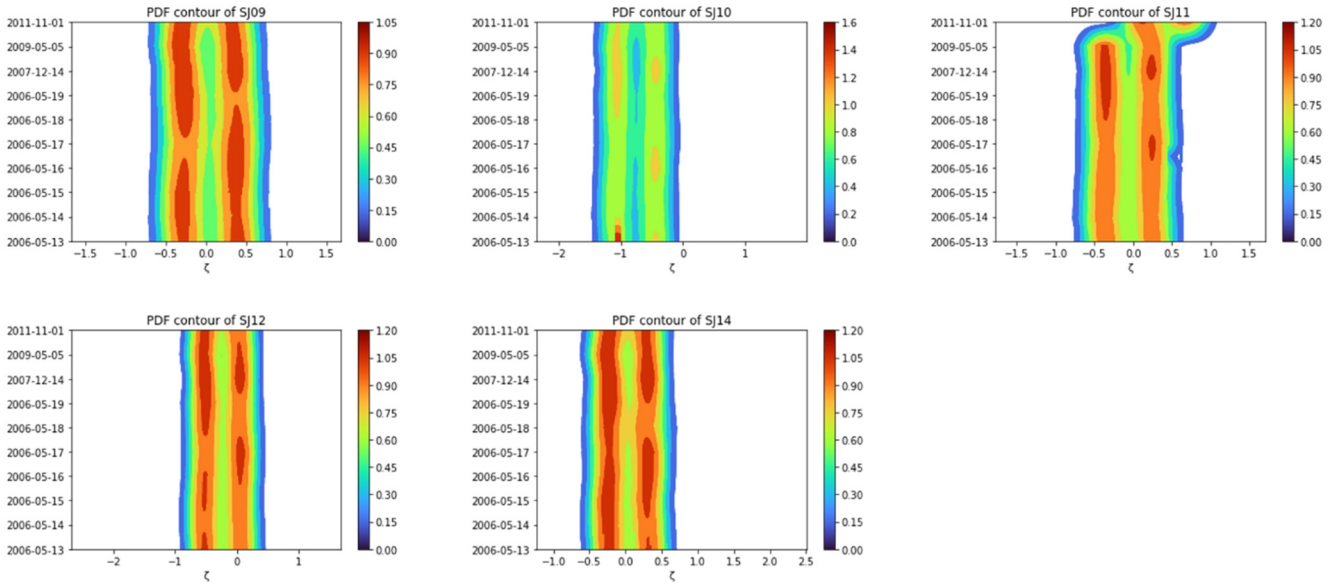

Fig. 10 PDF contours of cable pairs

SJS11 is always classified as the damaged cable in 2011-11-01 data, achieving 100% accuracy. It is noticed that that the clustering and deep learning methods did not classify SJS11 as the damaged cable in some cases. In Table 8, the LSTM correctly classified SJS11 when the damaged cable could not be classified correctly by the clustering (Hr: 01, 06, 09). Also, when the LSTM classified incorrectly (Hr: 03, 04, 05, 19~23), the clustering classified the damaged cable correctly, which indicates that the two approaches are complementary. Moreover, the cross-correlation method, which has the highest accuracy among the three methods, was also used for voting. Therefore, the individual classification of the three methods and combining the three methods are investigated. The combined classification denotes to identify the cable with the majority of the results from the three methods. It is seen that 100% accuracy is achieved by combining the three methods. Additionally, the existing one-class support vector machines (SVM), an outlier detection algorithm, is implemented for the comparison. The proposed methods have higher accuracies when comparing the SVM with the individually proposed methods and the combined classification. If the SVM is further optimized and four algorithms, including cross-correlation, clustering, deep learning, and SVM, are combined, a more stable outcome is obtained.

Furthermore, the technique of recognizing the tension ratio pattern is implemented for damage detection. The tension ratio of the facing cable pair and the Gaussian Mixture Model (GMM) are employed to calculate the tension ratio. Fig. 10 presents the PDFs derived by GMM as contour plots. The figure shows that the SJ11 pair (SJS11 and SJX11) has the mean value shift on 2011-11-01. The sudden shift in the mean value of GMM indicates that the cable is damaged. Therefore, it is inferred that SJS11 or SJX11 is damaged from the GMM technique. In addition, the insight from all techniques mentioned in this paper indicates that SJS11 is the damaged cable.

7. Conclusions

This paper proposed the combination method of three methodologies, including statistical modeling, clustering, and deep learning model to identify the damaged cables in the cable-stayed bridge. Firstly, the data records that interfered with the modeling were removed in the visual data search stage and substituted with the linear interpolations. Moreover, the data were preprocessed appropriately for each method to identify outliers. As the main task, the damaged cables were distinguished by comparing the data signal patterns. Then, the results by the STL decomposition model, cross-correlation, K-means time series clustering, and EncDec-AD were incorporated to identify the damaged cables. From all three approaches, SJS11 was identified as the damaged cable. The majority voting method was used to distinguish the damaged cable when the results differed from the three methods. In future work, the optimization of the clustering and deep learning algorithms will be considered. Moreover, voting techniques will be developed to identify damaged cables in the cable-stayed bridge.

Acknowledgments

This work was supported in part by the Basic Research Program through the National Research Foundation of Korea (NRF) funded by the MSIT under Grant 2019R1A4A1021702, and in part by Institute of Information & communications Technology Planning & Evaluation (IITP) grant funded by the Korea government (MSIT) (No.2021-0-02076, Developing Reasoning AI Engine in Complex Systems (REX) and its Applications).

References

Alamdari, M.M., Rakotoarivelo, T. and Khoa, N.L.D. (2017), "A spectral-based clustering for structural health monitoring of the Sydney Harbour Bridge", *Mech. Syst. Signal Process.*, **87**, 384-400. https://doi.org/10.1016/j.ymssp.2016.10.033

Bao, Y., Li, J., Nagayama, T., Xu, Y., Spencer Jr, B.F. and Li, H. (2021), "The 1st International Project Competition for Structural Health Monitoring (IPC-SHM, 2020): A summary and benchmark problem", *Struct. Health Monitor.*, **20**(4), 2229-2239. https://doi.org/10.1177/14759217211006485

Braga, P.L., Oliveira, A.L., Ribeiro, G.H. and Meira, S.R. (2007), "Bagging predictors for estimation of software project effort", *Proceedings of International Joint Conference on Neural Networks*, pp. 1595-1600. https://doi.org/10.1109/IJCNN.2007.4371196

Catbas, F.N., Gokce, H.B. and Gul, M. (2012), "Nonparametric analysis of structural health monitoring data for identification and localization of changes: Concept, lab, and real-life studies", *Struct. Health Monitor.*, **11**(5), 613-626. https://doi.org/10.1177/1475921712451955

Chae, J., Thom, D., Bosch, H., Jang, Y., Maciejewski, R., Ebert, D. and Ertl, T. (2013), "Spatiotemporal social media analytics for abnormal event detection and examination using seasonal-trend decomposition", *Proceedings of IEEE Conference on Visual Analytics Science and Technology* (*VAST*), Seattle, WA, USA, October, pp. 143-152. https://doi.org/10.1109/VAST.2012.6400557

Cleveland, R.B., Cleveland, W.S., McRae, J.E. and Terpenning, I. (1990), "STL: A seasonal-trend decomposition procedure based on loess", *J. Official Statist.*, **6**, 3-73.

Diez, A., Khoa, N.L.D., Alamdari, M.M., Wang, Y., Chen, F. and Runcie, P. (2016), "A clustering approach for structural health monitoring on bridges", *J. Civil Struct. Health Monitor.*, **6**, 429-445. https://doi.org/10.1007/s13349-016-0160-0

Duan, L., Xu, L., Liu, Y. and Lee, J. (2009), "Cluster-based outlier detection", *Ann. Oper. Res.*, **168**, 151-168. https://doi.org/10.1007/s10479-008-0371-9

Entezami, A., Sarmadi, H., Behkamal, B. and Mariani, S. (2020), "Big data analytics and structural health monitoring: a statistical pattern recognition-based approach", *Sensors*, **20**(8), p. 2328. https://doi.org/10.3390/s20082328

Gu, J., Gul, M. and Wu, X. (2017), "Damage detection under varying temperature using artificial neural networks", *Struct. Control Health Monitor.*, **24**, e1998. https://doi.org/10.1002/stc.1998

Hochreiter, S., and Schmidhuber, J. (1997), "Long short-term memory", *Neural Comput.*, **9**(8), 1735-1780. 10.1162/neco.1997.9.8.1735

Jiang, S.Y. and An, Q.B. (2008), "Clustering-based outlier detection method", *Proceedings of the 5th International Conference on Fuzzy Systems and Knowledge Discovery*, Jinan, China, October, Volume 2, pp. 429-433. https://doi.org/10.1109/FSKD.2008.244

Jo, H., Sim, S.H., Mechitov, K.A., Kim, R., Li, J., Moinzadeh, P., Spencer Jr, B.F., Park, J.W., Cho, S., Jung, H.J. and Yun, C.B. (2011), "Hybrid wireless smart sensor network for full-scale structural health monitoring of a cable-stayed bridge", *Proceedings of Sensors and Smart Structures Technologies for Civil, Mechanical, and Aerospace Systems 2011*, San Diego, CA, USA, March, Volume 7981, 798105. https://doi.org/10.1117/12.880513

Kingma, D.P. and Ba, J. (2015), "Adam: A method for stochastic optimization", *Proceedings of the 3rd International Conference on Learning Representations*, San Diego, CA, USA.

Lee, S. and Kim, H.K. (2018), "ADSaS: Comprehensive real-time anomaly detection system", Lecture Notes in Computer Science; In: *International Workshop on Information Security Applications*, pp. 29-41. https://doi.org/10.1007/978-3-030-17982-3_3

Li, S., Wei, S., Bao, Y. and Li, H. (2018), "Condition assessment of cables by pattern recognition of vehicle-induced cable tension ratio", *Eng. Struct*, **155**, 1-15. https://doi.org/10.1016/j.engstruct.2017.09.063

Malhotra, P., Ramakrishnan, A., Anand, G., Vig, L., Agarwal, P. and Shroff, G. (2016), "LSTM-based encoder-decoder for multi-sensor anomaly detection", *Proceedings of the ICML Anomaly Detection Workshop*, New York, NY, USA.

Mei, Q. and Gül, M. (2015), "Novel sensor clustering-based approach for simultaneous detection of stiffness and mass changes using output-only data", *J. Struct. Eng.*, **141**, p. 04014237. https://doi.org/10.1061/(ASCE)ST.1943-541X.0001218

Nair, K.K., Kiremidjian, A.S. and Law, K.H. (2006), "Time series-based damage detection and localization algorithm with application to the ASCE benchmark structure", *J. Sound Vib.*, **291**, 349-368. https://doi.org/10.1016/j.jsv.2005.06.016

Pamula, R., Deka, J.K. and Nandi, S. (2011), "An outlier detection method based on clustering", *Proceedings of the 2nd International Conference on Emerging Applications of Information Technology*, Kolkata, India, February, pp. 253-256. https://doi.org/10.1109/EAIT.2011.25

Paszke, A., Gross, S., Chintala, S., Chanan, G., Yang, E., DeVito, Z., Lin, Z., Desmaison, A., Antiga, L. and Lerer, A. (2017), "Automatic differentiation in pytorch", In: *NIPS 2017 Workshop Autodiff*.

Pathirage, C.S.N., Li, J., Li, L., Hao, H. and Liu, W. (2018), "Application of deep autoencoder model for structural condition monitoring", *J. Syst. Eng. Electro.*, **29**, 873-880. https://doi.org/10.21629/JSEE.2018.04.22

Sutskever, I., Vinyals, O. and Le, Q.V. (2014), "Sequence to sequence learning with neural networks", In: *Advances in Neural Information Processing Systems*, pp. 3104-3112.

Theodosiou, M. (2011), "Forecasting monthly and quarterly time series using STL decomposition", *Int. J. Forecast.*, **27**(4), 1178-1195. https://doi.org/10.1016/j.ijforecast.2010.11.002

Tian, Y., Xu, Y., Zhang, D. and Li, H. (2020), "Relationship modeling between vehicle-induced girder vertical deflection and cable tension by BiLSTM using field monitoring data of a cable-stayed bridge", *Struct. Control Health Monitor.*, **28**(4), p. e2667. https://doi.org/10.1002/stc.2667

Xingjian, S.H.I., Chen, Z., Wang, H., Yeung, D.Y., Wong, W.K. and Woo, W.C. (2015), "Convolutional LSTM network: A machine learning approach for precipitation nowcasting", In: *Advances in Neural Information Processing Systems*, pp. 802-810.

Yu, L. and Lin, J.C. (2017), "Cloud computing-based time series analysis for structural damage detection", *J. Eng. Mech.*, **143**, C4015002. https://doi.org/10.1061/(ASCE)EM.1943-7889.0000982

Zhang, Y., Meratnia, N. and Havinga, P. (2010), "Outlier detection techniques for wireless sensor networks: A survey", *IEEE Commun. Surveys Tutorials*, **2**, 159-170. https://doi.org/10.1109/SURV.2010.021510.00088

Zhang, C., Song, D., Chen, Y., Feng, X., Lumezanu, C., Cheng, W., Ni, J., Zong, B., Chen, H. and Chawla, N.V. (2019), "A deep neural network for unsupervised anomaly detection and diagnosis in multivariate time series data", *Proceedings of the AAAI Conference on Artificial Intelligence*, Honolulu, HI, USA, January-February, Volume 33, pp. 1409-1416. https://doi.org/10.1609/aaai.v33i01.33011409